is grateful for the award of an NSERC postgraduate scholarship.

Registry No. **1**, 101630-10-8; **2**, 101630-11-9; **3**, 101630-12-0; **4**, 101630-13-1; **5**, 101630-14-2; **6**, 101630-15-3; **7**, 101630-16-4; **8**, 101630-17-5; *cis*-$Mo(CO)_4(C_5H_{11}N)_2$, 65337-26-0; *cis*-$W(CO)_4(C_5H_{11}N)_2$, 56083-13-7; $NiCl_2(PPh_3)_2$, 14264-16-5; $PdCl_2(PPh_3)_2$, 13965-03-2; *cis*-$PtCl_2(PPh_3)_2$, 15604-36-1; Ni, 7440-02-0; Pd, 7440-05-3; Pt, 7440-06-4; W, 7440-33-7; Mo, 7439-98-7.

Supplementary Material Available: Tables SI-SIII listing thermal parameters, the derived hydrogen positions, and angles and distances associated with the phenyl and cyclohexyl rings (5 pages). Ordering information is given on any current masthead page. According to policy instituted Jan 1, 1986, the tables of calculated and observed structure factors (21 pages) are being retained in the editorial office for a period of 1 year following the appearance of this work in print. Inquiries for copies of these materials should be directed to the Editor.

Contribution from the Department of Chemistry,
York University, North York, Ontario M3J 1P3, Canada

Comparative Spectra and Kinetics of Ferrous Bis(dioxime) Complexes of π-Acid Ligands

Nafees Siddiqui and Dennis V. Stynes*

Received October 14, 1985

Syntheses, visible spectra, and kinetic data for axial ligand dissociation for low-spin *trans*-FeN_4XY complexes (N_4 = bis(benzoquinone dioxime) (BQDH), bis(naphthoquinone dioxime) (NPQH); X, Y = methylimidazole, tributylphosphine, tributyl phosphite, benzyl isocyanide, carbon monoxide) are reported and compared with corresponding dimethylglyoxime (DMGH) analogues. MLCT bands in both NPQH and BQDH derivatives are red-shifted up to 200 nm from those in corresponding DMGH complexes, and all show shifts as a function of axial ligands that correlate with π-acceptor character. Infrared data and CO dissociation rates indicate an axial π-back-bonding order DMGH > NPQH > BQDH. The NPQH complexes have labilities comparable to those of DMGH analogues but several orders of magnitude slower than those of BQDH complexes. All three systems give the trans-effect series MeIm > PBu_3 > $P(OBu)_3$ > BzNC > CO (except PBu_3 > MeIm for BQDH complexes). The three systems provide a set of over 50 different complexes whose dissociative thermal substitution reactions are fully characterized and that display photochromism based on photochemical substitution in solution covering the entire visible region of the spectrum.

Introduction

Kinetic investigations of axial ligand substitution in a variety of low-spin iron(II) complexes of the general form *trans*-FeN_4LT, where N_4 is a planar tetradentate ligand and L and T are monodentate ligands, have established a dissociative mechanism. The system N_4 = bis(dimethylglyoxime) has been the most extensively studied, and correlations in reactivity with the MLCT band have been observed.[2,3] An analogous benzoquinone dioxime system[4] displays a 200-nm shift of the MLCT band and exhibits kinetic and spectroscopic properties for carbonyl and isocyanide complexes that are substantially different from those of the DMGH analogues. Previous studies of naphthoquinone dioxime complexes of iron without consideration of the axial ligands present have been reported.[5-7]

Herein we present a comparison of the spectroscopic and kinetic parameters for benzoquinone dioxime, naphthoquinone and dimethylglyoxime complexes containing methylimidazole, pyridine, tributylphosphine, tributyl phosphite, benzyl isocyanide, and carbon monoxide as axial ligands. A systematic analysis of the labilization effects in these three systems provides a basis for understanding the reactivity of low-spin d^6 complexes and insight into the even greater lability of hemes.

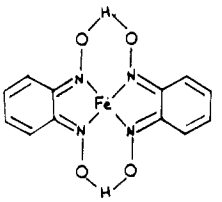

BQDH

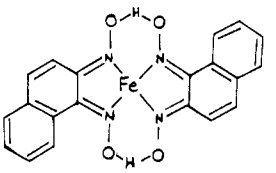

NPQH

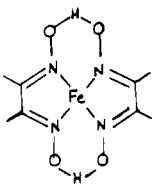

DMGH

Results and Discussion

Data for the BQDH and NPQH complexes generally follow trends similar to those for the DMGH system described in detail previously.[2] Species show characteristic MLCT spectra, and axial ligand substitution reactions are readily followed by visible spectroscopy, providing overwhelming evidence for a classic dissociative mechanism. The rate constants, all obtained in toluene solution, provide fundamental information about the metal-axial ligand bonding and its dependence on the *cis*-N_4 ligand and trans ligand. Activation parameters show these effects to be largely enthalpic and not very sensitive to solvation effects.

Visible Spectra. The visible spectra of iron bis(dioxime) derivatives are dominated by an intense MLCT band assigned to metal d(*xz*,*yz*) to oxime charge transfer.[8] Substantial shifts in this band are observed as extended conjugation in the oxime ligand

(1) Abbreviations: DMGH, dimethylglyoximate; BQDH, benzoquinone dioximate; NPQH, naphthoquinone dioximate; MeIm, 1-methylimidazole; Im, imidazole; BzNC, benzyl isocyanide; TMIC, (*p*-tolylsulfonyl)methyl isocyanide; py, pyridine, 4-CN-py, 4-cyanopyridine; 3,4-Me_2-py, 3,4-dimethylpyridine; 4-Me_2N-py, 4-(dimethylamino)-pyridine; MLCT, metal to ligand charge transfer. Rate constants are designated by k^T_{-L} for dissociation of the ligand L trans to T. The shortened forms N (MeIm), P (PBu_3), and PO ($P(OBu)_3$) are used as subscripts and superscripts.

(2) (a) Pang, I. W.; Stynes, D. V. *Inorg. Chem.* **1977**, *16*, 59. (b) Chen, X.; Stynes, D. V. *Inorg. Chem.*, in press.
(3) Vaska, L.; Yamaji, T. *J. Am. Chem. Soc.* **1971**, *93*, 6673.
(4) Pomposo, F.; Stynes, D. V. *Inorg. Chem.* **1983**, *22*, 569.
(5) Toel, K.; Motomizu, S.; Kuse, S. *Anal. Chim. Acta* **1975**, *75*, 323.
(6) Marvel, G. S.; Porter, P. K. *Organic Syntheses*; Wiley: New York, 1950; Collect Vol. II, p 411.
(7) Nasakkala, M.; Saarinen, H.; Korvenranti, J.; Nasakkala, E. *Acta Chem. Scand., Ser. A* **1977**, *A31*, 469.
(8) Yamano, Y.; Masuda, I.; Shinra, K. *Bull. Chem. Soc. Jpn* **1971**, *44*, 1581.

0020-1669/86/1325-1982$01.50/0

Table I. Visible Spectral Data for FeN_4LT Complexes: λ_{max} (nm), in Toluene Solution

L	T	DMGH[a]	NPQH	BQDH
MeIm	MeIm	531	702, 410	755, 440[b]
	PBu_3	499	642, 406	680, 440
	$P(OBu)_3$	460	591, 396	612, 440
	BzNC	445	567, 404	582, 430[b]
	TMIC	428	545, 395	560, 440
	CO	385	474, 380	485, 400[b]
PBu_3	PBu_3	468	594, 402	616, 440
	$P(OBu)_3$	436	558, 390	570, 428
	BzNC	425	542, 380	556, 422
	CO	376	470, 380	475, 400
$P(OBu)_3$	$P(OBu)_3$	414	527, 380	537, 420
	BzNC	399	515, 376	520, 412
	CO	360	455, 373	
BzNC	BzNC	392	505, 400	515, 412[b]
	CO	350		485, 400
py	py	508, 417	655, 390, 356 sh	704, 420, 375
	PBu_3	492, 374	635, 405	
	$P(OBu)_3$	459, 368	586, 395	504
	CO	389, 350		484, 400[b]
4-CN-py	4-CN-py	496, 530	638, 493	680, 460 sh, 440
4-NMe_2-py	4-NMe_2-py	554, 330	730, 412, 350 sh	772, 444
3,4-Me_2-py	3,4-Me_2-py	514, 407	680	724, 440

[a] Reference 2. [b] λ_{max} values for these were previously reported in $CHCl_3$ solution.[4] In some cases the band is shifted slightly in toluene.

Table II. MLCT Shifts (cm^{-1}) with Changes in Axial Ligands

X	N_4 DMGH	N_4 NPQH	N_4 BQDH
A. Energy of MLCT for FeN_4(MeIm)(X)–Energy of MLCT for FeN_4(MeIm)$_2$			
PBu_3	1208	1331	1461
$P(OBu)_3$	2907	2675	3095
BzNC	3640	3392	3937
CO	7142	6852	7374
B. Energy of MLCT for FeN_4X_2–Energy of MLCT for FeN_4(MeIm)(X)			
PBu_3	1328	1259	1528
$P(OBu)_3$	2416	2055	2282
BzNC	3079	2165	2659
C. Energy of MLCT for $FeN_4(py)_2$–Energy of MLCT for FeN_4X_2			
4-NMe_2-py	−1634	−1339	−1252
3,4-Me_2-py	−343	−332	−393
4-CN-py	476	336	501

is introduced. The band is also sensitive to the nature of the axial ligands shifting to higher energy as ligands of increased π-acceptor strength are introduced that lower d(xz,yz). Extensive data for all three systems are tabulated in Table I. The BQDH complexes have MLCT bands at about 5000 cm^{-1} lower energy than those of DMGH analogues and at slightly lower energy than those of NPQH complexes. The presence of an additional aromatic ring in NPQH apparently reduces the extent of interaction with the oxime chromophore. The NPQH and BQDH complexes also show a band at ~400 nm that does not shift appreciably with axial ligands and is assigned to a ligand band.

The shifts in the MLCT band with axial ligand are given in Table II in units of cm^{-1}. The shifts are remarkably similar in the three systems, with increasing values as the π-acceptor strength of the axial ligand increases. The effect is reduced somewhat if the trans ligand is also a good π acceptor (PBu_3 is an exception possibly because of its strong σ-bonding ability). The BQDH system shows the largest shifts in all cases with MeIm as the trans ligand.

In pyridine derivatives an additional band is observed that is sensitive to substituents on the pyridine ring. This band is assigned to charge transfer to pyridine and occurs at about 500 ± 40 nm for the FeN_4(4-CN-py)$_2$ and at about 350 ± 30 nm for the FeN_4(4Me_2N-py)$_2$ complexes. This band also shifts to higher energy in FeN_4(py)(X) species, where X is a π acceptor, and occurs in a region which is difficult to assign.

Table III. IR Data: ν_{CO} and ν_{NC} (cm^{-1})[a]

	T	DMGH[c]	NPQH	BQDH[d]	heme[c]	Pc[c]
FeN_4CO	py	1985	2010			1995[b]
FeN_4CO	MeIm	1978		2028[b]	1970	1995[b]
FeN_4BzNC	py	2145				
FeN_4BzNC	MeIm	2141	2158	2170	2149	2160
FeN_4BzNC	BzNC	2167		2184		2180

[a] Nujol mull unless stated otherwise; T is ligand trans to CO or BzNC. [b] Chloroform solution. [c] Reference 2a. [d] Reference 4.

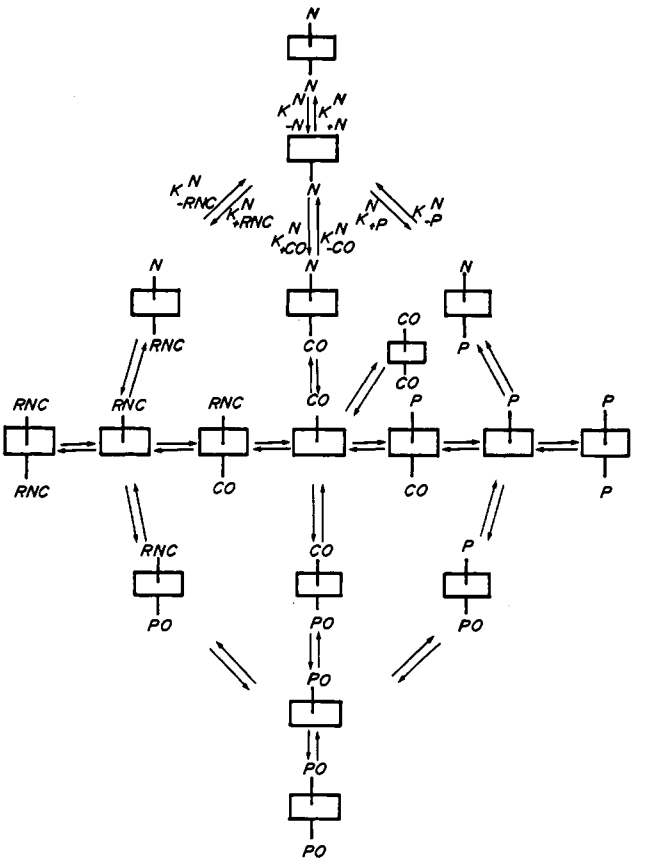

Figure 1. Reaction scheme showing the reactions of the 13 complexes FeN_4XY and 5 pentacoordinate intermediates for the 5 different ligands MeIm (N), PBu_3 (P), $P(OBu)_3$ (PO), BzNC (RNC), and Co. The symbolism used for on- and off-rate constants is indicated for the trans ligand N. The two species FeN_4(PO)(N) and FeN_4(P)(CNR) are omitted for clarity.

The charge-transfer to pyridine band occurs at highest energy in the BQDH system, occurring at ~3000 cm^{-1} higher energy than the DMGH analogue in FeN_4(4-CN-py)$_2$. This result indicates that d(xz,yz) lies at somewhat lower energy in Fe(BQDH)$_2$ complexes than in corresponding NPQH and DMGH analogues. We attribute this to increased π interaction between iron and the BQDH ligand. The shifts in the charge transfer-to-4-CN-py band do not support an argument for extensive π-acceptor character for 4-CN-py since this would lead to the greatest transition energy in the DMGH system, where other evidence suggests axial π back-bonding is greatest. In fact, the opposite is true. We interpret the shifts in metal to oxime charge transfer with pyridine basicity as arising from global σ effects. The trends in the CT to pyridine then correlate with lowering of d(xz,yz) as a result of increased iron to oxime π bonding. This feature is probably the dominant factor in the differences between the BQDH system and NPQH and DMGH analogues.

Infrared Spectra. IR data for CO and NC stretching frequencies are compared in Table III. The values of ν_{CO} and ν_{NC} are generally taken as evidence of π-bonding effects. The data

Table IV. Trans-Effect Summary in the Naphthoquinone System: $k^{T}_{-L} \times 10^{4}$ (s^{-1}) in Toluene

		trans ligand, T			
k^{T}_{-L}	temp, °C	MeIm	PBu_3	$P(OBu)_3$	BzNC
k_{-N}	25	17			
	45	275	13	0.17	
	60	1730	95	1.9	
	70		340	7.6	
	90				6.3
k_{-P}	60	1.3	1.1		
	70	4.0	4.1		
	80	21	17	0.25	
k_{-PO}	45	2.8			
	60	26	21	2.3	
	70	83		9.4	
	80			35	
k_{-BzNC}	45	0.4			
	60	3.6	5.8	0.17	
	70	16	22		
	80		70		
k_{-CO}	25	3.7	140	15	
	40	31			
	50	100			
k_{-py}	25	740[a]	31	0.28	

[a] Trans to py.

Table V. Trans-Effect Summary in $Fe(BQDH)_2LT$ Complexes: $k^{T}_{-L} \times 10^{3}$ (s^{-1}) in Toluene

		trans ligand, T			
k^{T}_{-L}	temp, °C	MeIm	PBu_3	$P(OBu)_3$	BzNC
k_{-N}	−23	...	1.45		
	10	60[a]	...	2.2	
	25	...	...	16.5	0.068
	45				1.5
	60				10
k_{-P}	10	0.024	1.0	...	
	25	0.27	10	...	
	45	4.1	110	3.0	0.03
k_{-PO}	10	0.3		0.53	
	25	3.3	50	5.5	
	45	44		7.0	0.41
k_{-BzNC}	25	0.31	5.9	0.3	
	45	5.8	86		0.13
	60	33			
k_{-CO}	0		160		
	10	2.0			1.1

[a] 10% chloroform in toluene; these results are similar to values previously reported[4] in pure chloroform.

show the axial π-back-bonding ability DMGH > NPQH > BQDH. This order is understood as arising from reduced axial π-basicity of iron as the iron to oxime π bonding increases. Thus the BQDH system shows the highest ν_{CO} and ν_{NC} values and weakest axial π-bonding because of extensive π interaction of $d(xz,yz)$ with the oxime π orbitals. Evidence for this interaction is found in the charge-transfer bands cited above. The value of k^{N}_{-CO} also correlates with the π-bonding order deduced from IR data. Data for hemes and phthalocyanine complexes are included for comparison.

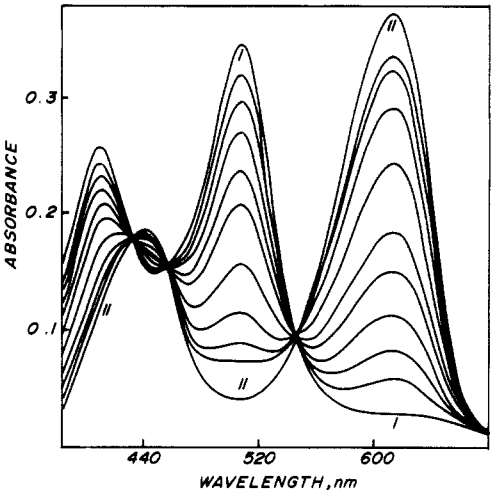

Figure 2. Spectral changes with time following addition of 0.1 M PBu_3 to a toluene solution of $Fe(BQDH)_2(BzNC)_2$ at 45 °C. Spectra 1–10 are at times 0, 10, 20, 33.3, 53, 73, 118, 174, 229, and 267 min, respectively. The final spectrum 11 was obtained by photolysis. A clean reaction to give $Fe(BQDH)_2(PBu_3)_2$ is observed at a rate k^{BzNC}_{-BzNC} without evidence for the intermediate $Fe(BQDH)_2(PBu_3)(BzNC)$.

Kinetics. The general reaction scheme is shown in Figure 1.

Reactions of the NPQH and BQDH complexes proceed generally as previously found for the DMGH analogues.[2] For the reaction

$$FeN_4TL + E \rightarrow FeN_4TE + L \qquad (1)$$

for leaving group L, trans ligand T, and entering ligand E, a pseudo-first-order rate constant k_{obsd} is obtained by monitoring the visible spectrum with time. Under conditions where [E] >> [L], $k_{obsd} = k^{T}_{-L}$ is independent of the concentration or nature of the entering ligand. These "off rates" are summarized in Tables IV and V with activation parameters collected in Table VI. For the reaction

$$FeN_4L_2 + E \xrightarrow{k_1} FeN_4LE \rightarrow FeN_4E_2 \qquad (2)$$

where L is much less labilizing than E, a single rate processes (k_1) is detected with clean isosbestic points with no evidence for the middle species. The typical case L = BzNC and E = PBu_3 is shown in Figure 2. When L and E have comparable trans effects, two consecutive first-order rates are observed such as shown in Figure 3, L = $P(OBu)_3$ and E = MeIm. When L is significantly delabilizing with respect to E, two distinctly separate rate processes, each with clean isosbestics, are observed as shown in Figure 4.

Table VI. Activation Parameters[a] for Dissociation of L Trans to T in $Fe(dioxime)_2LT$ Complexes in Toluene

	DMGH[b]			NPQH			BQDH		
	$\Delta H^{\ddagger}$, kcal/mol	$\Delta S^{\ddagger}$, cal/(deg mol)	$\Delta G^{\ddagger}$, kcal/mol	$\Delta H^{\ddagger}$, kcal/mol	$\Delta S^{\ddagger}$, cal/(deg mol)	$\Delta G^{\ddagger}$, kcal/mol	$\Delta H^{\ddagger}$, kcal/mol	$\Delta S^{\ddagger}$, cal/(deg mol)	$\Delta G^{\ddagger}$, kcal/mol
k^{N}_{-N}	25.7	17.0	20.5	25.5	14.2	21.2			
k^{P}_{-N}	29.5	21.3	23.1	27.7	15.0	23.2			
k^{PO}_{-N}	30.9	19.3	25.2	32.5	21.0	26.2			
k^{BzNC}_{-N}	31.0	12.0	27.4				27.6	15.0	23.1
k^{N}_{-P}	32.5	25.3	25.0	32.0	19.0	25.6	25.7	11.2	22.4
k^{P}_{-P}				31.3	17	26.7	23.4	10.6	20.2
k^{N}_{-PO}	29.0	18.4	24.0	29.0	16.1	24.2	24.9	13.4	20.9
k^{PO}_{-PO}				31.2	18.1	25.8	24.3	12.4	20.6
k^{N}_{-BzNC}				31.3	19.4	25.5	25.8	12.0	22.2
k^{P}_{-BzNC}				28.5	11.9	24.9			
k^{N}_{-CO}	27	7.0	24.8	24.9	8.8	22.1	23[c]	10[c]	20[c]

[a] Estimated errors: $\Delta H^{\ddagger}$, ±1 kcal/mol; $\Delta S^{\ddagger}$, ±4 cal/(deg mol). [b] Reference 2. [c] $CHCl_3$ solution.[4]

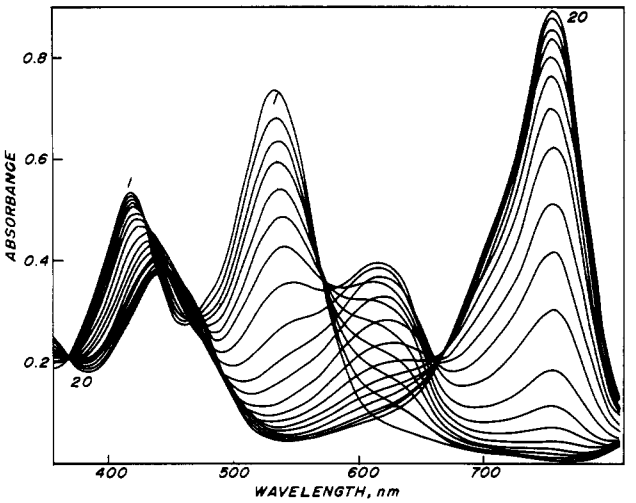

Figure 3. Spectral changes with time following addition of 0.4 M MeIm to a toluene solution of $Fe(BQDH)_2(P(OBu)_3)_2$ at 10 °C. Two consecutive first-order rates were obtained: $k^{PO}_{-PO} = 5.8 \times 10^{-4}$ s^{-1}; $k^{N}_{-PO} = 3.2 \times 10^{-4}$ s^{-1}. The intermediate $Fe(BQDH)_2(MeIm)(P(OBu)_3)$, $\lambda_{max} = 616$ nm, reaches its maximum concentration after about 50 min.

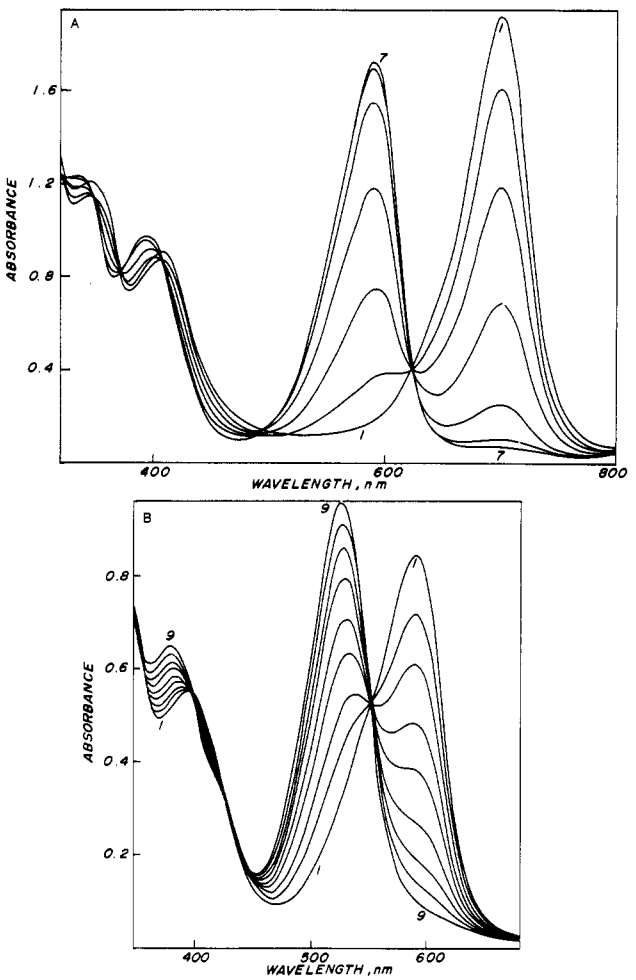

Figure 4. (A) Spectral changes with time following addition of 0.1 M $P(OBu)_3$ to a toluene solution of $Fe(NPQH)_2(MeIm)_2$ at 25 °C: (1) before addition; (2–7) at times 0, 3, 9, 21, 38, and 66 min, respectively. $Fe(NPQH)_2(MeIm)(P(OBu)_3)$ is formed at the rate k^{N}_{-N}. (b) Spectral changes with time at 70 °C for the slower second step following that shown in Figure 4A. Times for spectra 1–9 are 0, 4, 8, 14, 20, 30, 42, 57, and 87 min, respectively. $Fe(NPQH)_2(P(OBu)_3)_2$ is formed at the rate k^{PO}_{-N}.

The mixed-ligand species were typically generated in situ by making use of kinetic or equilibrium control of the reaction solution. These species are characterized on the basis of their

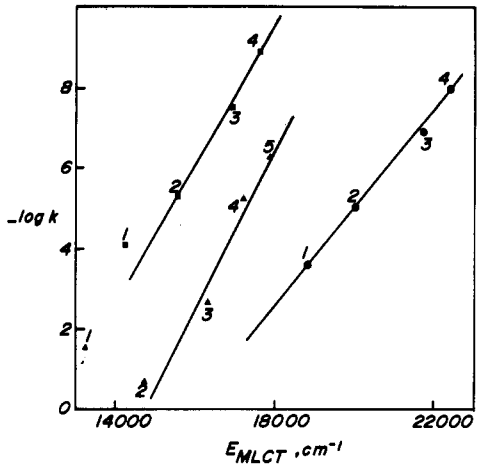

Figure 5. Correlation of dissociation rates (k^{T}_{-N} at 10 °C) of MeIm trans to T with E_{MLCT}: (1) T = MeIm; (2) T = PBu_3; (3) T = $P(OBu)_3$; (4) T = BzNC; (5) T = TMIC; (■) NPQH; (▲) BQDH; (●) DMGH. All data are extrapolated to 10 °C with use of activation parameters.

characteristic visible spectra and the interrelation and established rates in the global scheme shown in Figure 1.

For example, the species $Fe(NPQH)_2(P(OBu)_3)(CO)$ could be generated thermally at 80 °C in CO-saturated toluene at the rate k^{PO}_{-PO} or photochemically at 10 °C. The product generated by either method reacted with excess $P(OBu)_3$ to give $Fe(NPQH)_2(P(OBu)_3)_2$ at the rate k^{PO}_{-CO} or with excess ligand E to give $FeN_4(P(OBu)_3)(E)$, E = MeIm, PBu_3, BzNC. These products $FeN_4(P(OBu)_3)E$ undergo further reactions in a slower step at the rate k^{E}_{-PO}, giving FeN_4E_2. The species $FeN_4(P(OBu)_3)(E)$ can also be generated by a variety of other routes and the rates k^{E}_{-PO} obtained as indicated in Figure 1.

As in the DMGH system, in no case is direct replacement of any ligand trans to CO observed. Relative rates of addition to the pentacoordinate intermediates were not obtained in this work, since they are expected to closely parallel the small differences found in the DMGH system.[2] The very slow reactions involving loss of ligands trans to BzNC in the NPQH system were not investigated here since the analogous data is available in the DMGH complexes.

The kinetic data, trans effects, and leaving-group order for the NPQH system are remarkably similar to those of the corresponding DMGH system reported previously. No reaction studied has a $\Delta G^{\ddagger}$ value more than about 1 kcal/mol different from that of the corresponding DMGH reaction, except those involving loss of CO. Trans to MeIm, CO is 2.6 kcal/mol more inert in $\Delta G^{\ddagger}$ in the DMGH system, indicative of greater axial π-bonding in the DMGH complexes.

The trans-effect order in both DMGH and NPQH complexes for loss of σ donors is

$$MeIm > PBu_3 > P(OBu)_3 > BzNC$$

with the magnitude of the effects decreasing as the leaving group becomes a better π acceptor and a partial reversal of the order for the strong π acceptor CO. In the BQDH system, the corresponding trans-effect order is

$$PBu_3 > MeIm > P(OBu)_3 > BzNC$$

The anomaly in the trans-effect series for BQDH is seen to be in the position of MeIm. For example, PBu_3 is about 30 times more labile trans to PBu_3 compared to trans to $P(OBu)_3$ in both BQDH and NPQH systems. Similarly $P(OBu)_3$ is about 10 times more labile trans to PBu_3 vs. $P(OBu)_3$ in both systems. However, dissociation of PBu_3 is 25 times faster trans to PBu_3 vs. MeIm in BQDH but has comparable lability trans to either PBu_3 or MeIm in the NPQH system. We attribute these differences to a greater emphasis on σ-donor properties of the axial ligand in the BQDH system.

A correlation of the dissociation rate of MeIm with the MLCT energy previously found for the DMGH system[2] is also observed

Table VII. Comparison of Lability of Ligands in Iron Complexes: $\Delta G^{\ddagger}_{298}$ (kcal/mol) Trans to MeIm[a]

leaving group	N_4				
	heme	BQDH	NPQH	DMGH	Pc
MeIm	13.1[c]	17.7	21.2	20.5	21.0
$P(OBu)_3$	15.1[b,f]	20.9	24.2	23.3	22.5[e]
PBu_3	15.9[b,f]	22.4	25.6	25	23.5[f]
BzNC	17.9[d]	22.2	25.5	25	23.1
CO	19.6	20.0	22.1	24.7	19.8

[a] All data in toluene solution unless otherwise noted; in cases where activation parameters are unknown, extrapolations to 298 K were made by assuming $\Delta S^{\ddagger}$ has the average value of those given in Table VI for this system. [b] Calculated from equilibrium constants for hemin diester assuming rate ratios $k_{+N}/k_{+P} = 4$[2] and $k^{N}_{-N} = 1500\ s^{-1}$.[14] [c] Tetraphenylporphyrin, in benzene solution.[14] [d] Value for BuNC in benzene;[15] this is expected to be similar to that of BzNC. [e] Martinsen, J.; Miller, M.; Trojan, D.; Sweigart, D. A. *Inorg. Chem.* **1982**, *19*, 2162. [f] Fletcher, D.; Stynes, D. V., unpublished results.

in NPQH and BQDH complexes. The observed linear correlation is no doubt to some extent fortuitous since both E_{MLCT} and k^{T}_{-N} depend on σ- and π-bonding properties of the trans ligand T. If π-bonding effects are dominant, a correlation is anticipated if a substantial loss in this π bonding to T occurs on loss of MeIm (as expected on the basis of a synergistic trans interaction) since E_{MLCT} largely reflects the lowering of d(xz,yz) as a result of axial π bonding. All three systems give remarkably good linear correlations; however, the location of MeIm is increasingly above (more inert) the correlation line in the order DMGH < NPQH < BQDH.

The trans effect of MeIm was generally found to be out of line in the BQDH system above. This effect may arise from the ability of the BQDH ligand to remove electron density from iron and thus decrease the destabilizing effect of two strong axial σ donors. Alternatively, a good axial σ donor may enhance π-bonding to the BQDH ligand in a cis effect.

The trans effects on CO dissociation are of interest since one expects that π-bonding effects would play a dominant role. The general trans-labilizing order for CO loss is $PBu_3 > P(OBu)_3 >$ BzNC $\geq$ MeIm, which clearly does not correlate with π-bonding, steric, or σ-donor effects alone.

Except for the position of MeIm, the trans-effect order for loss of CO is the same as that found for loss of all of the other ligands studied. This suggests that even when a very good π acceptor is lost, the predominant trans effect involves the ability of the trans ligand to donate electrons and stabilize the 16-electron intermediate.[9] Good donors stabilize the transition state and give fast rates; poor donors destabilize and give slow rates. Only the nitrogen bases pyridine and MeIm violate this principle, and then only in complexes with very strong π acceptors. This may be due to substantial ground-state stabilization that occurs for a trans MeIm or pyridine. This ground-state stabilization of CO is reflected in the well-known dependence of ν_{CO} on the trans ligands. For example, Timney's[10] ligand-effect constants suggest the ground-state stabilization order MeIm or Py >> $PBu_3 \approx$ BzNC > $P(OBu)_3$ for a CO ligand. The trans-effect order for CO loss presumably reflects a compromise between ground-state stabilization and transition-state stabilization, both of which increase with net donor strength but give opposite kinetic effects. For leaving groups of lesser π-acceptor strength than CO, the transition-state stabilization effect dominates the trans-effect order.

In addition to the difference in the trans-effect order, the BQDH system is substantially more labile than DMGH and NPQH complexes. In Table VI for example, both $\Delta H^{\ddagger}$ and $\Delta G^{\ddagger}$ are typically 2–6 kcal/mol lower in reactions of BQDH compared to those values in NPQH complexes. The largest labilizing effects occur when MeIm is the trans ligand because of the different trans effects discussed above.

This general pattern of increased lability for *all* ligands is also found in hemes. Values of $\Delta G^{\ddagger}_{298}$ for the three oxime systems, iron phthalocyanine, and iron porphyrins are given in Table VII for loss of various ligands trans to MeIm. Clearly none of the four systems show the lability typical of hemes. Only for k^{N}_{-CO} do some of the models approach the lability in hemes, and this is accomplished largely via strong π bonding with N_4, which is probably not the source of CO lability in hemes. (ν_{CO} is not as high in hemes as in BQDH.) What is apparent is that the heme system provides a mechanism for lowering $\Delta G^{\ddagger}$ for σ donors as well as π acceptors that is not duplicated in any of the other four systems, although the BQDH system comes the closest.

Photochemical Applications. All three oxime systems display photosubstitution reactions similar to that of other FeN_4 systems[11-13] in solution in the presence of excess ligands, photochromism is observed on the basis of the shift of the equilibrium

$$FeN_4TL + E \rightleftharpoons FeN_4TE + L \qquad (3)$$

As an example, for the case N_4 = NPQH, T = $P(OBu)_3$, L = CO, and E = $P(OBu)_3$ one can reversibly drive the above equilibrium to the right by irradiation at 455 nm or drive it to the left by irradiation at 527 nm.

With all of the pertinent thermal rates determined for these complexes, an extensive array of relatively inert low-spin d^6 iron complexes is now available for exploring MLCT photochemistry in the visible region of the spectrum. Details of the photochemistry of these systems will be published elsewhere.[12]

Experimental Section

Materials. $Fe(BQDH)_2(MeIm)_2$, $Fe(BQDH)_2(py)_2$ and $Fe(BQDH)_2(BzNC)_2$ were available from previous work.[4] $NPQH_2$ was prepared from 1-nitroso-2-naphthol[6] by a literature method.[7]

Physical Measurements. Visible spectra were recorded on an Aminco DW-2a UV/vis spectrophotometer. NMR spectra were obtained on a Bruker AM300 instrument with an Aspec 3000 computer, using deuteriochloroform as solvent with 0.1–0.5% Me_4Si as internal standard. Elemental analyses were performed by Canadian Microanalytical Service Ltd., Vancouver, BC, Canada.

Syntheses. All syntheses were carried out under a nitrogen atmosphere. Solid samples gave satisfactory elemental analysis.

$Fe(NPQH)_2(MeIm)_2$. Naphthoquinone dioxime (1 g) and $FeSO_4 \cdot 7H_2O$ (3 g) were heated to boiling for 15 min in 100 mL of $CHCl_3$, containing 1 mL of MeIm and 20 mL of benzene, to give a bright green solution. The resulting mixture was filtered to remove excess $FeSO_4$, and the volume was reduced in vacuo. Hexane was added, giving a green precipitate, which was recrystallized twice from $CHCl_3$/hexane and dried in vacuo; yield 1 g. NMR: δ 3.4 (MeIm, CH_3); 6.37, 7.06 (MeIm, CH); 6.7, 7.3–9.7 (NPQH). Visible: $\epsilon = 2.5 \times 10^4$ at λ = 702 nm.

$Fe(NPQH)_2(py)_2$ was prepared similarly with use of pyridine in place of methylimidazole.

The following were prepared by methods analogous to those in ref 2 and gave satisfactory elemental analyses and NMR spectra indicated below.

NMR for $Fe(NPQH)_2(PBu_3)_2$: δ 0.63 (PBu_3, $-CH_3$); 1.0 (PBu_3, CH_2); 1.25 (PBu_3, CH_2); 6.7, 9.6, 9.7 ($(NPQH)_2$).

NMR of $Fe(NPQH)_2(P(OBu)_3)_2$: δ 0.89 ($P(OBu)_3$, CH_3); 1.33–1.65 m ($P(OBu)_3$), CH_2); 3.6 ($P(OBu)_3$), OCH_2); 6.7, (2 H) 7.3 (8 H), 9.59 (2 H) (NPQH).

NMR for $Fe(NPQH)_2(MeIm)(BzNC)$: δ 3.46 (MeIm, CH_3), 4.58 (Bz, CH_2); 6.57 (MeIm, CH); 6.7–7.78 (m) (Bz, MeIm, and NPQH); 9.64, 9.66 (NPQH).

$Fe(BQDH)_2(PBu_3)_2$ and $Fe(BQDH)_2(P(OBu)_3)_2$ were prepared from $Fe(BQDH)_2(py)_2$ by the methods described for the analogous $Fe(DMGH)_2$ complexes.[2]

NMR for $Fe(BQDH)_2(PBu_3)_2$: δ 0.69 (PBu_3, CH_3); 0.94 (PBu_3, CH_2); 1.0 (PBu_3, CH_2); 6.4, 7.1, 7.2 (BQDH).

In Situ Generation of Species. Species generated in situ at $\sim 10^{-4}$ M in toluene were in all cases products of a clean reaction with known rates monitored by visible spectroscopy. λ_{max} is in Table I. Procedures for the

(9) Atwood, J. D.; Wovkulich, J. J.; Sonnenberger, D. C. *Acc. Chem. Res.* **1983**, *16*, 350.
(10) Timney, J. A. *Inorg. Chem.* **1979**, *18*, 2502.
(11) Irwin, C.; Stynes, D. V. *Inorg. Chem.* **1978**, *17*, 2882.
(12) Chen, X.; Stynes, D. V., to be submitted for publication.
(13) Butler, A.; Linck, R. G. *Inorg. Chem.* **1984**, *23*, 4545.
(14) Lavallette, D.; Tetreau, C.; Momenteau, M. *J. Am. Chem. Soc.* **1979**, *101*, 5395.
(15) Olson, J. S.; McKinnie, R. E.; Mims, M. P.; White, D. K. *J. Am. Chem. Soc.* **1983**, *105*, 1522.

NPQH derivatives were essentially identical with those previously reported for the DMGH analogues.[2]

Corresponding procedures for the BQDH analogues were similar except that the reactions were generally run at 25 °C or lower owing to the faster rates (see Table III). For $Fe(BQDH)_2(MeIm)(PBu_3)$ a variation in procedure was required owing to the trans effect $PBu_3 > MeIm$ in this system. For the determination k^N_{-P} an excess of MeIm (300 μL) was added to 3 mL of a stock solution of $Fe(BQDH)_2(PBu_3)_2$. The initial fast reaction to give $Fe(BQDH)_2(MeIm)(PBu_3)$ was complete in seconds, and the subsequent slower reaction was monitored with time. For the determination of k^P_{-N} at −23 °C, solid $Fe(BQDH)_2(MeIm)_2$ was dissolved in a toluene solution containing 10^{-4} M PBu_3 and 7.5×10^{-4} M MeIM and the mixture was left to stand until a spectrum containing primarily $Fe(BQDH)_2(MeIm)(PBu_3)$ with ~20% $Fe(BQDH)_2(PBu_3)_2$ and negligible $Fe(BQDH)_2(MeIm)_2$ was obtained. Excess PBu_3 was then added to obtain k^P_{-N} independent of $[PBu_3]$ from 0.025 to 0.1 M.

Kinetics. Reactions in which CO was the entering ligand were carried out under 1 atm of CO. Otherwise, all reactions were routinely run in serum-capped nitrogen-purged cuvettes and monitored by visible spectroscopy. Temperatures were maintained by means of water circulation through a thermostatable cell holder. Temperatures were read directly from an RTD device attached to the cell holder.

Reaction solutions were prepared by injecting either the ligand (either by itself or as a toluene solution) into a dilute solution of the complex or the more concentrated solution of the complex into a thermostated toluene solution of the ligand.

In all cases rates were found to be invariant to a 10-fold variation of the entering ligand (typically 0.03–0.3 M). Reactions for species generated in situ were always carried out with the entering ligand in at least 50-fold excess over the leaving ligand. Complex concentrations for kinetic runs were typically 10^{-4} M or less.

Rate constants for reactions involving a single pseudo-first-order rate were obtained from a least-squares fit of $\log [(A - A_\infty)/(A_0 - A_\infty)]$ vs. time using a microcomputer analysis as described elsewhere.[2] For reactions involving two consecutive first-order rates of comparable magnitude, absorbance data vs. time at several wavelengths were analyzed by computer comparison of observed and calculated absorbance as described previously.[2] Photolyses were carried out with white light or 100 Å band-pass interference filters.

Acknowledgment. Support of the National Sciences and Engineering Research Council of Canada is gratefully acknowledged.

Contribution from the Department of Chemistry,
University of Victoria, Victoria, British Columbia, Canada V8W 2Y2

^{31}P and ^{195}Pt NMR Studies and the Crystal and Molecular Structure of Chloro(triethylphosphine)[tris(diphenylphosphinothioyl)methyl]platinum(II), $[PtCl(PEt_3)\{C(PPh_2S)_3\}]$, an S,S-Bonded Chelate with Dynamic Stereochemistry Controlled by One Labile and One Inert Pt–S Bond

Jane Browning, Kathryn Anne Beveridge, Gordon William Bushnell, and Keith Roger Dixon*

Received September 25, 1985

Reaction of $CH(PPh_2S)_3$ with $[Pt_2Cl_4(PEt_3)_2]$ or $[Pt_2Cl_2(PEt_3)_4][BF_4]_2$ results in spontaneous deprotonation of the ligand to form $[PtCl(PEt_3)\{C(PPh_2S)_3\}]$ (I) or $[Pt(PEt_3)_2\{C(PPh_2S)_3\}][BF_4]$ (II), respectively. Compound I crystallizes as a dichloromethane solvate in the monoclinic space group $P2_1/c$, with a = 16.902 (3) Å, b = 13.999 (2) Å, c = 19.771 (3) Å, and β = 93.03 (2)°, and the structure was refined to R = 0.0561 (R_w = 0.0725) by using 3635 independently measured reflections. The square-planar platinum coordination involves only two of the sulfur atoms (Pt–S = 2.282 (3) and 2.351 (4) Å), and the methanide carbon is closely planar with P–C–P angles from 116.2 (7) to 124.2 (7)°. In solution at temperatures above ca. 50 °C, I undergoes a dynamic intramolecular process in which the noncoordinated sulfur exchanges with the coordinated sulfur trans to triethylphosphine. The Pt–S bond trans to chloride remains inert and serves as a pivot for the exchange process. The differing Pt–S bond strengths implied by this process are reflected in both the bond lengths, 2.282 (3) Å trans to Cl and 2.351 (4) Å trans to P, and in the two-bond Pt–P NMR coupling constants, 128 and 48 Hz, respectively. Compound II undergoes a related exchange process except that both Pt—S bonds are labilized by trans phosphine ligands and all three P═S groups of the ligand are involved in the exchange. ^1H, $^{13}C\{^1H\}$, $^{31}P\{^1H\}$, and $^{195}Pt\{^1H\}$ NMR spectra are reported for both complexes, and the exchange processes are studied in detail by ^{31}P NMR to yield $\Delta G^{\circ\ddagger}$ values of 67.1 and 61.3 kJ mol^{-1} for I and II, respectively.

Introduction

The ligands $CH(PPh_2)_3$, $CH(PPh_2S)_3$, and $[C(PPh_2S)_3]^-$ have attracted recent attention.[1-4] For example, the ability of a polydentate ligand to maintain the integrity of a cluster unit during a catalytic reaction is of obvious interest, and complexes in which $CH(PPh_2)_3$ coordinates to a triangular cluster face have been reported.[1] Although this is also possible in principle for the sulfur derivatives, it appears that their coordination chemistry is rather different. Thus in reactions with Hg(II) or Cd(II) salts, coordination of $CH(PPh_2S)_3$ is accompanied by deprotonation to form complexes in which $[C(PPh_2S)_3]^-$ functions as a uninegative, tridentate ligand toward a single metal center.[2,3] Related complexes of Cu(I), Ag(I), and Au(I) can be prepared by reactions of metal salts with $[n\text{-}Bu_4N][C(PPh_2S)_3]$.[4] This behavior is similar to that found for the well-known tripyrazolylborates, which appear to be the only previous examples of this rather rare class of ligands.[5,6] However, whereas some complexes of the tripyrazolylborates exhibit a bidentate, fluxional coordination mode, for example in $[Pd(\eta\text{-}C_3H_5)(HB(pz)_3)]$,[5,6] only the tridentate mode has been reported to date for $[C(PPh_2S)_3]^-$.

We have recently reported a novel coordination mode for a closely related ligand, $[CH(PPh_2S)_2]^-$. In the complex $[PtCl(PEt_3)\{CH(PPh_2S)_2\}]$ this ligand is a C,S-bonded chelate, but in solution at ambient temperature the coordinated and noncoordinated P═S groups undergo continuous dynamic interchange.[7] It was therefore of considerable interest to investigate the platinum complexes of $CH(PPh_2S)_3$ and $[C(PPh_2S)_3]^-$ to determine whether these exhibit any coordination modes other than the tridentate coordination found in the metal complexes described above. The present paper describes the results of this study. The complexes are S,S-bonded chelates that exhibit dynamic, intramolecular interchange of coordinated and noncoordinated P═S groups. The nature of the interchange and the site at which it occurs are

(1) Bahsoun, A. A.; Osborn, J. A.; Voelker, C.; Bonnet, J. J.; Lavigne, G. *Organometallics* **1982**, *1*, 1114.
(2) Grim, S. O.; Smith, P. H.; Satek, L. C. *Polyhedron* **1982**, *1*, 137.
(3) Grim, S. O.; Nittolo, S.; Ammon, H. L.; Smith, P. H.; Colquhoun, I. J.; McFarlane, W.; Holden, J. R. *Inorg. Chim. Acta* **1983**, *77*, L241.
(4) Grim, S. O.; Sangokoya, S. A.; Gilardi, R. D.; Colquhoun, I. J.; McFarlane, W. Presented at the 23rd International Conference on Coordination Chemistry; Boulder, CO, 1984.
(5) Trofimenko, S. *Acc. Chem. Res.* **1971**, *4*, 17.
(6) Trofimenko, S. *Chem. Rev.* **1972**, *72*, 497.
(7) Browning, J.; Bushnell, G. W.; Dixon, K. R.; Pidcock, A. *Inorg. Chem.* **1983**, *22*, 2226.

0020-1669/86/1325-1987$01.50/0